

Preparation of Ti_3C_2 -modified ZnFe_2O_4 photocatalytic materials and their performance in degrading tetracycline in water

Section S1: Chemicals and reagents.

Titanium aluminum carbide powder ($\text{Ti}_3\text{AlC}_2 > 98\%$, 200 mesh, Foshan Ene Technology Co., LTD), hydrofluoric acid ($\text{HF} \geq 40\%$, Shanghai Maclin Biochemical Technology Co., Ltd.), dimethyl sulfoxide ($\text{DMSO} \geq 99\%$, Shanghai Maclin Biochemical Technology Co., Ltd.), Zinc acetate ($\text{Zn}(\text{AC})_2 \cdot 2\text{H}_2\text{O} \geq 99.0\%$, Tianjin Kemi Ou Chemical Co., Ltd.), Ferric chloride hexahydrate ($\text{FeCl}_3 \cdot 6\text{H}_2\text{O}$, Shanghai Wokai Biotechnology Co., Ltd.), sodium hydroxide ($\text{NaOH} \geq 96.0\%$, Chengdu Jinshan Chemical Co., Ltd.), Disodium ethylenediamine tetraacetate ($\text{EDTA-2Na} \geq 99.0\%$, Shanghai Sobao Biotechnology Co., Ltd.), p-benzoquinone ($\text{C}_6\text{H}_4\text{O}_2$, 99%, Shanghai Aladdin Reagent Co., Ltd.), ethylene glycol ($(\text{CH}_2\text{OH})_2$, 98%, Shanghai Aladdin Reagent Co., Ltd.), Isopropyl alcohol ($(\text{CH}_3)_2\text{CHOH}$, 99.7%, Tianjin Fuyu Fine Chemical Co., Ltd.), Tetracycline hydrochloride ($\text{C}_{22}\text{H}_{24}\text{N}_2\text{O}_8 > 96\%$, Shanghai Alding Reagent Co., Ltd.), deionized water, anhydrous ethanol. Reagents and chemicals are analytical grade and require no further purification for use.

Section S2: Synthesis of Ti_3C_2 .

According to the literature report ¹, the preparation plan of Ti_3C_2 is shown in the text. 2.5 g Ti_3AlC_2 is taken, a small amount of Ti_3AlC_2 is slowly added into 60 mL HF within 5 minutes for etching, and the Al layer is removed by stirring at room temperature (25°C) for 72 h, and then filtered through the sand core funnel device. The products were washed with deionized water and anhydrous ethanol successively until the PH of the washing liquid was about neutral. The filtered products were put into a vacuum drying oven at 60°C for 12 h. The dried black powder was added into 50 mL DMSO for intercalation, stirred at room temperature for 24 h, filtered through sand core funnel device, washed with deionized water and anhydrous ethanol, and dried overnight in a vacuum drying oven at 60°C . Finally, multilayer Ti_3C_2 black powder was obtained.

Section S3: Synthesis of ZnFe_2O_4 and $\text{Ti}_3\text{C}_2/\text{ZnFe}_2\text{O}_4$

Based on the literature ², a series of $\text{Ti}_3\text{C}_2/\text{ZnFe}_2\text{O}_4$ photocatalytic materials and a single ZnFe_2O_4 photocatalytic material were synthesized by hydrothermal method. $\text{Ti}_3\text{C}_2/\text{ZnFe}_2\text{O}_4$ composites with a mass ratio of 1.5/1, 1/1, 0.5/1, 0.25/1 and 0.2/1 were prepared with Ti_3C_2 of different qualities, that is, a certain amount of Ti_3C_2 MXenes was added to 20 mLEG, and the

black Ti_3C_2 was completely dispersed in EG after ultrasonic for 20 min. Then 0.1352 g $\text{FeCl}_3 \cdot 6\text{H}_2\text{O}$ was added into the mixture, and the mixture was continued to be ultrasounded for 10 min to form A black brown homogeneous viscous solution A. The transparent thick solution B was obtained by dissolving 0.0549 g $\text{Zn}(\text{AC})_2 \cdot 2\text{H}_2\text{O}$ in 10 mL EG for 10 min. Under the condition of intense stirring of solution A, solution B was added to solution A at the rate of 1 drop/s (while stirring). After the drip was added, the reaction was carried out at the same speed for 30 min, and the PH of the solution was adjusted slowly with 1 mol/L NaOH until the PH was 11, and then the solution was stirred vigorously for 1 h. Finally, the obtained solution was transferred to a 100 mL polytetrafluoroethylene high-pressure reactor and reacted at 160°C for 6 h. After removal, the product was cooled to room temperature, washed with deionized water and anhydrous ethanol for 3 times, and dried overnight in a vacuum drying oven at 60°C . Finally, the brown product $\text{Ti}_3\text{C}_2/\text{ZnFe}_2\text{O}_4$ was obtained. (The preparation of ZnFe_2O_4 is the same as the preparation of $\text{Ti}_3\text{C}_2/\text{ZnFe}_2\text{O}_4$ in other steps and conditions except that no Ti_3C_2 is added)

Section S4: Photocatalytic activity evaluation

The photocatalytic activities of Ti_3C_2 , ZnFe_2O_4 and $\text{Ti}_3\text{C}_2/\text{ZnFe}_2\text{O}_4$ series photocatalysts were evaluated for TCH degradation under simulated visible light irradiation were investigated. Typically, 20 mg of the as-prepared catalyst was added to a TCH solution (100 mL, $20 \text{ mg} \cdot \text{L}^{-1}$). The solution was stirred continuously at 350 rpm in the dark for 30 min to reach adsorption-desorption equilibrium. After simulated sunlight illumination generated by a 300 W Xe lamp (Alpha-1860A, Shanghai Spectral Element Instrument Co., Ltd. output wavelength 420–780 nm), 3 mL of the suspension was removed and filtrated through a $0.22 \mu\text{m}$ filter every 10 min and detected using a UV–vis spectrophotometer at $\lambda = 356 \text{ nm}$. All the degradation experiments were conducted at a constant room temperature (25°C). The catalyst was recovered via centrifugation with water and anhydrous ethanol for recycling.

Section S5: Characterization.

The crystal structures of all the samples were analysed by X-ray diffractometer (XRD, BRUKERD 8A DVANCE) at a scanning rate of 5 min^{-1} in the 2θ range of $5\text{--}90^\circ$. XPS analysis of the chemical state of materials is carried out on X-ray photoelectron spectrometer (Thermo ESCALAB 250) to obtain the surface element composition and bonding laws of the materials. The binding energy of the sample was calibrated using 284.6 eV as reference line. The field emission scanning electron microscope (FESEM) images were collected by Zeiss EVO25 microscope to observe the morphology of the samples. The chemical structures of

Ti₃C₂, ZnFe₂O₄ and Ti₃C₂/ZnFe₂O₄ series photocatalytic materials have been studied by Fourier transform infrared spectroscopy (FTIR). UV–vis diffuse reflectance spectra (DRS) were recorded at room temperature with a Shimadzu UV 3600 UV–vis spectrophotometer. Electron spin resonance spectrometer (ESR, Bruker A300) was used to detect oxygen vacancy and free radical generation. Electrochemical experiments were conducted with CHI600E electrochemical workstation (Chenhua Instrument) to characterize photocurrent and obtain electrochemical impedance spectroscopy (EIS). Fluorescence spectrophotometer (FLS980 Edinburgh Instruments) is used to measure the photoluminescence (PL) and time-resolved photoluminescence (TR-PL) emission spectrum. TOC–LCPH (Elementer vario Toc titrator) was used for total organic carbon analysis.

Section S6: Analysis of intermediates.

The degradation intermediates during TCH degradation were analysed using an LC–MS (Agilent–1290II–6460, U.S. Agilent Technologies Inc.) system equipped with an SP–C18 chromatographic column. The mobile phase was 0.5% formic acid (HCOOH) and acetonitrile in a volume ratio of 0.3:0.7 with a flow rate of 0.3 mL·min⁻¹. The injection volume was 20.00 μL, and the column temperature was 30 °C.

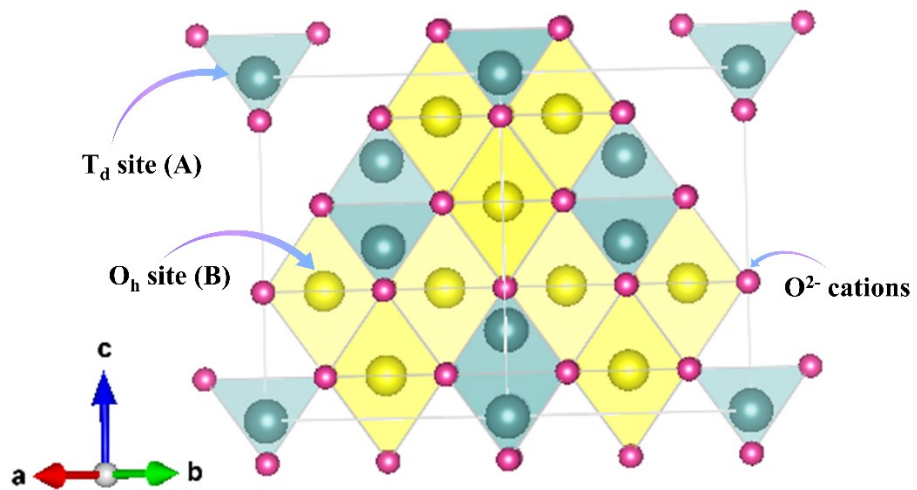


Fig. S1. Crystal structure of spinel crystals. Blue and yellow represent metal cations at T_d and O_h, respectively, while oxygen ions are marked in rose red ³.

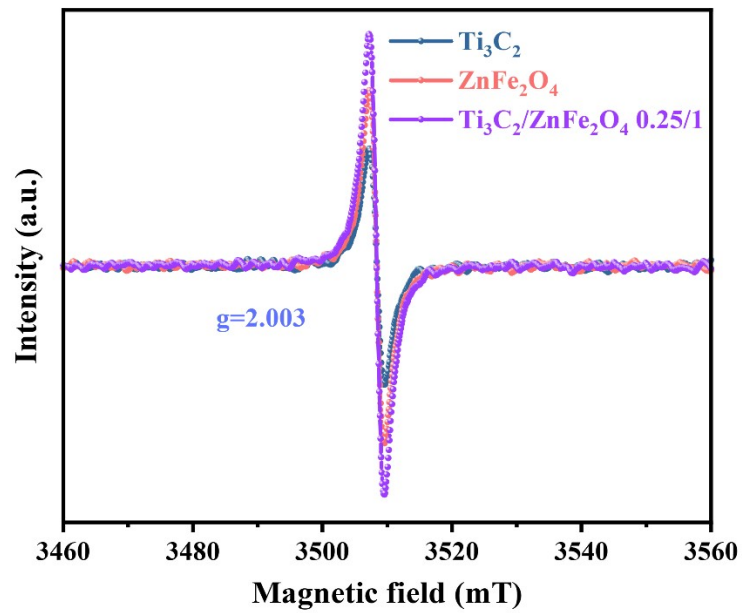


Fig. S2. ESR spectra of Ti_3C_2 , ZnFe_2O_4 and the 0.25/1 $\text{Ti}_3\text{C}_2/\text{ZnFe}_2\text{O}_4$ samples.

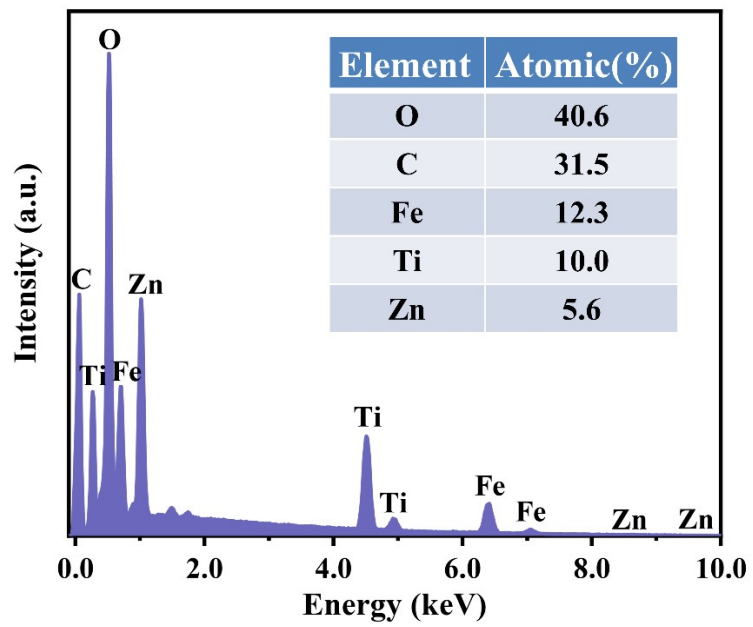


Fig. S3. EDS spectrum of 0.25/1 $\text{Ti}_3\text{C}_2/\text{ZnFe}_2\text{O}_4$.

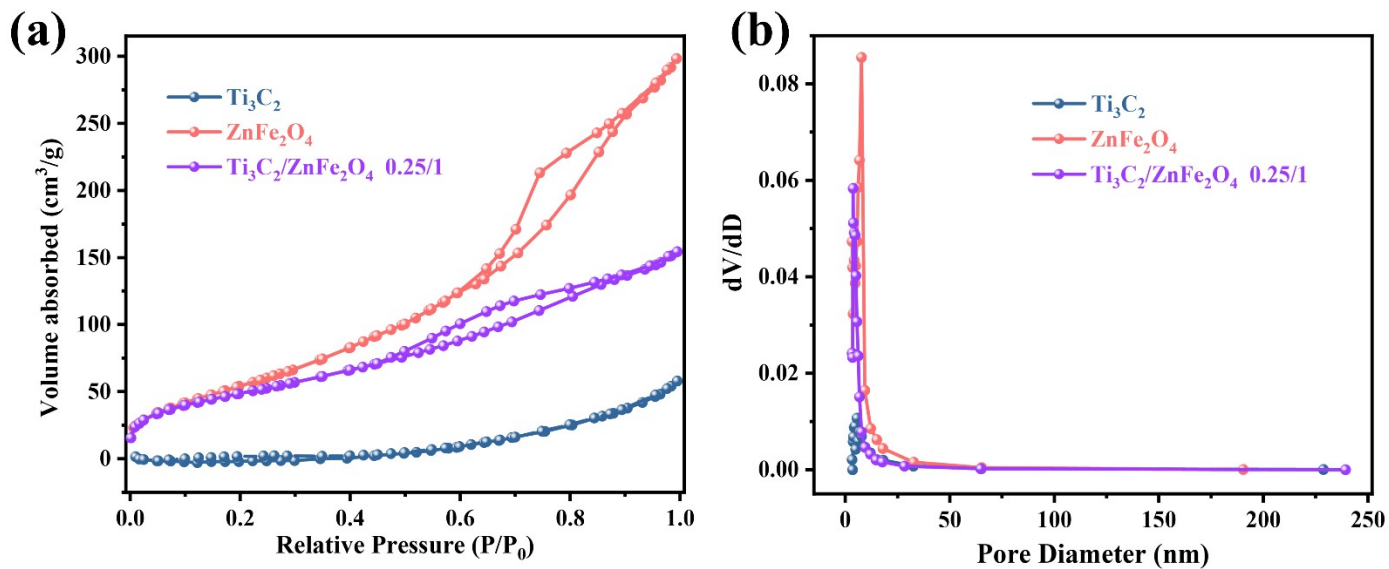


Fig. S4. (a) N₂ adsorption–desorption isotherms and (b) Barrett–Joyner–Halenda (BJH) pore size distribution of Ti₃C₂, ZnFe₂O₄ and the 0.25/1 Ti₃C₂/ZnFe₂O₄ samples.

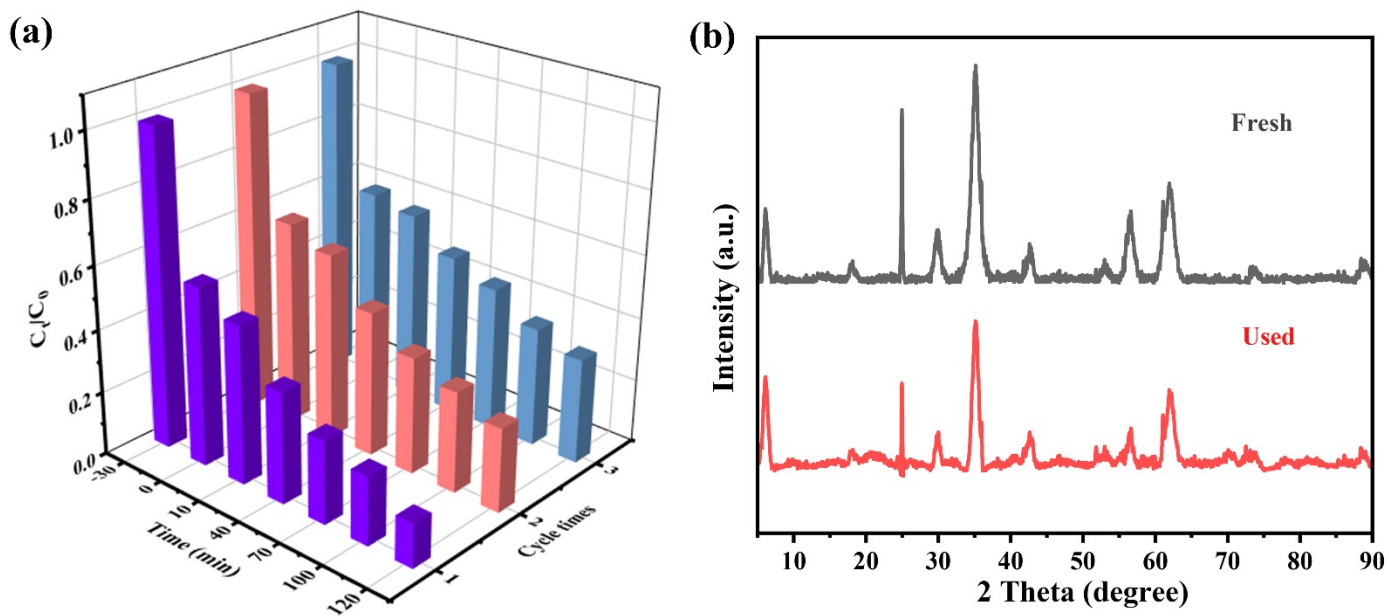


Fig. S5. (a) Cycling runs for photocatalytic TCH degradation in the presence of 0.25/1 $\text{Ti}_3\text{C}_2/\text{ZnFe}_2\text{O}_4$, and (b) XRD patterns of fresh and recycled 0.25/1 $\text{Ti}_3\text{C}_2/\text{ZnFe}_2\text{O}_4$ catalyst.

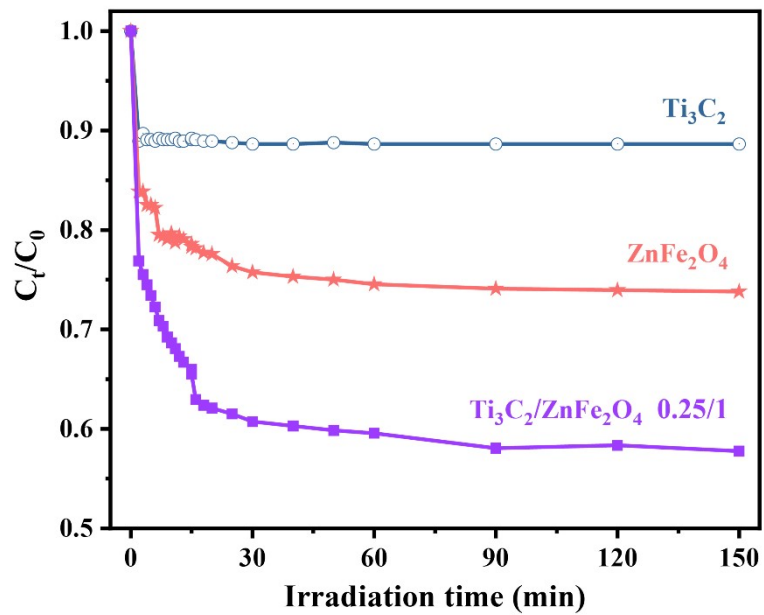
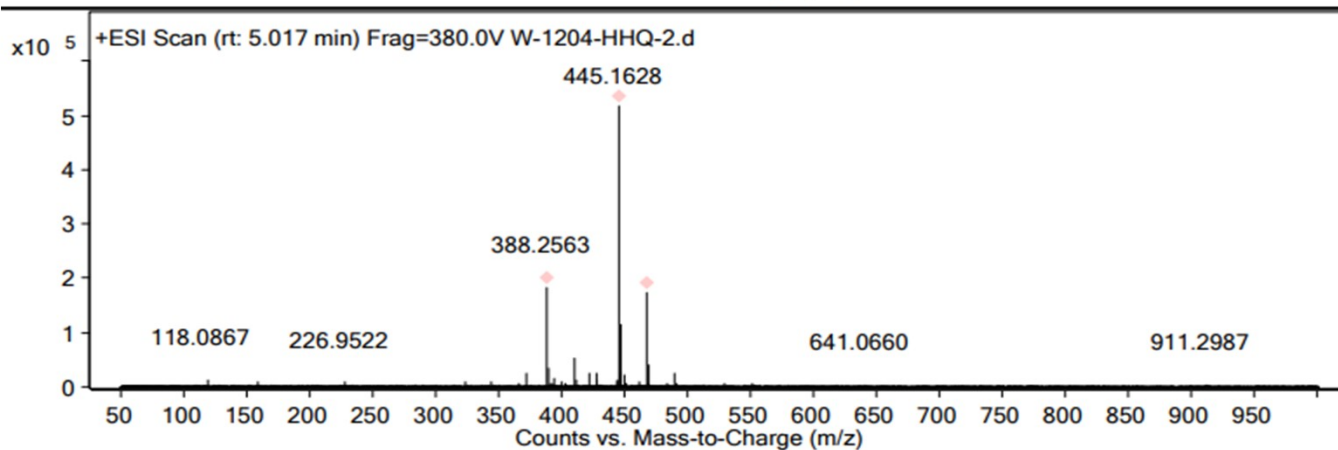
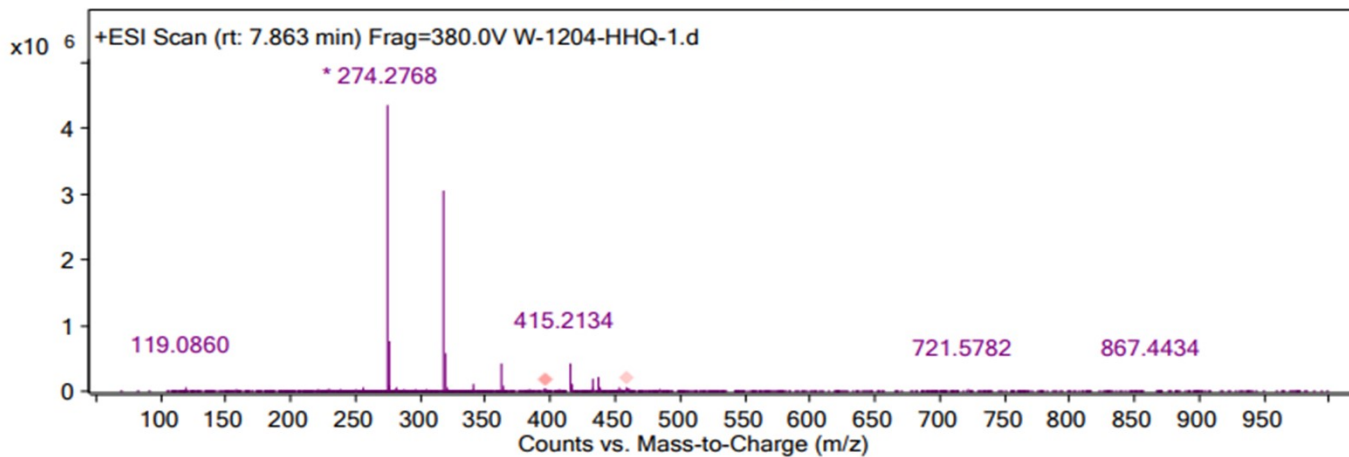
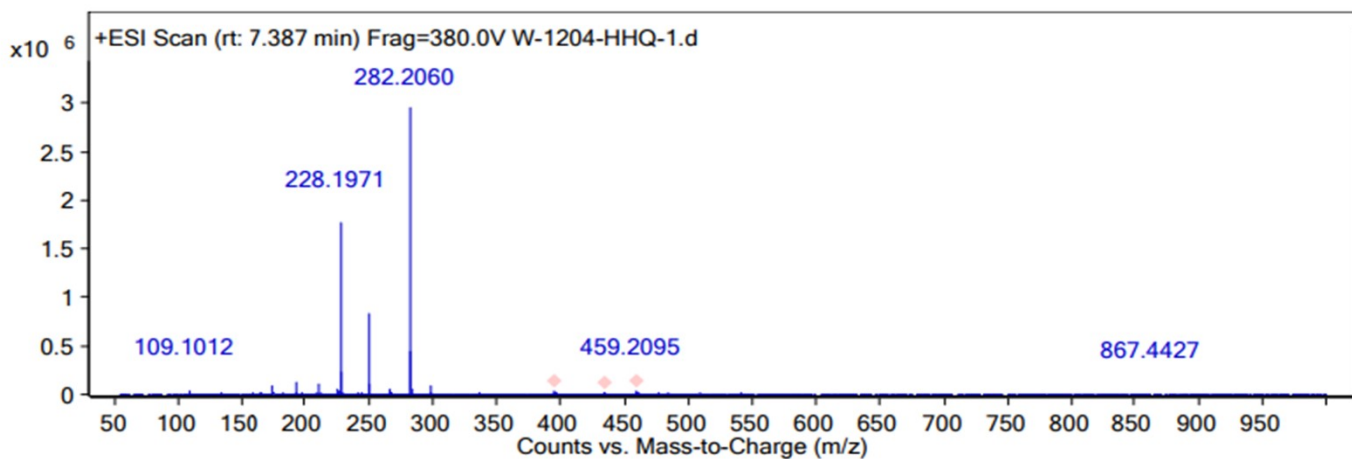
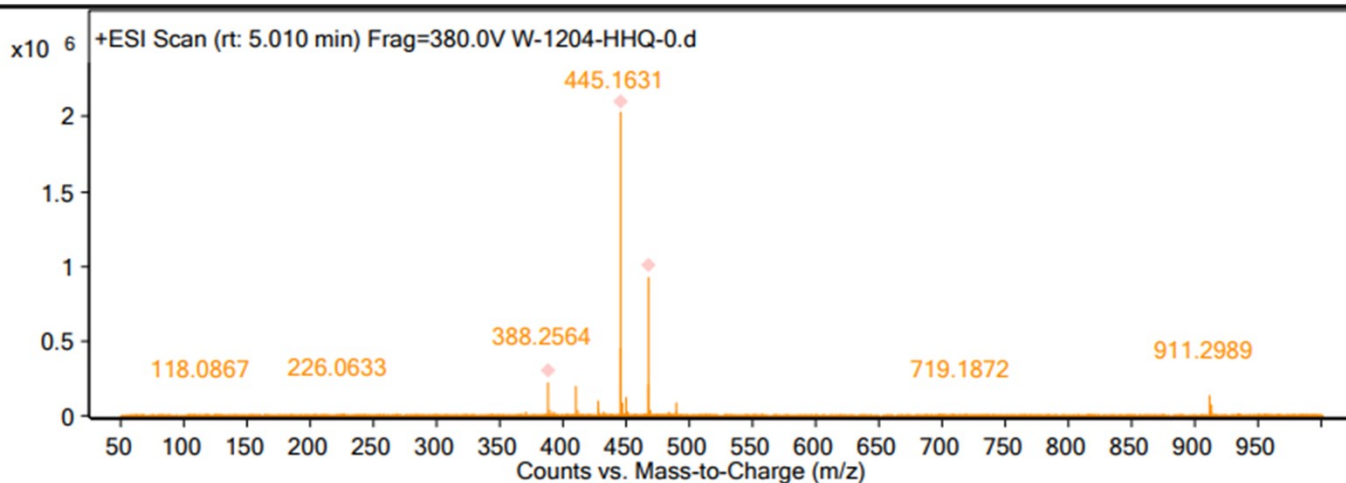
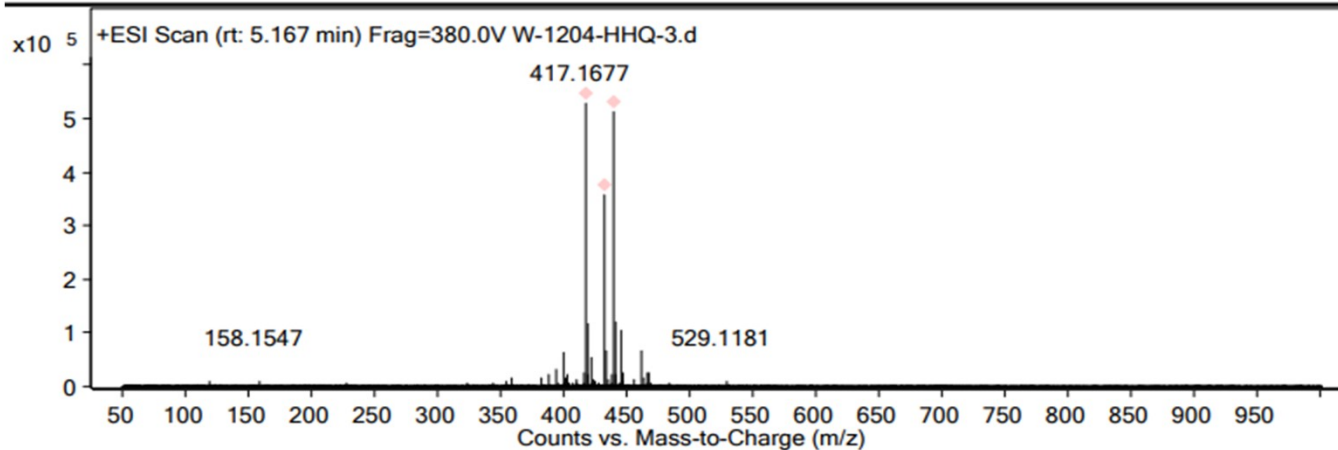
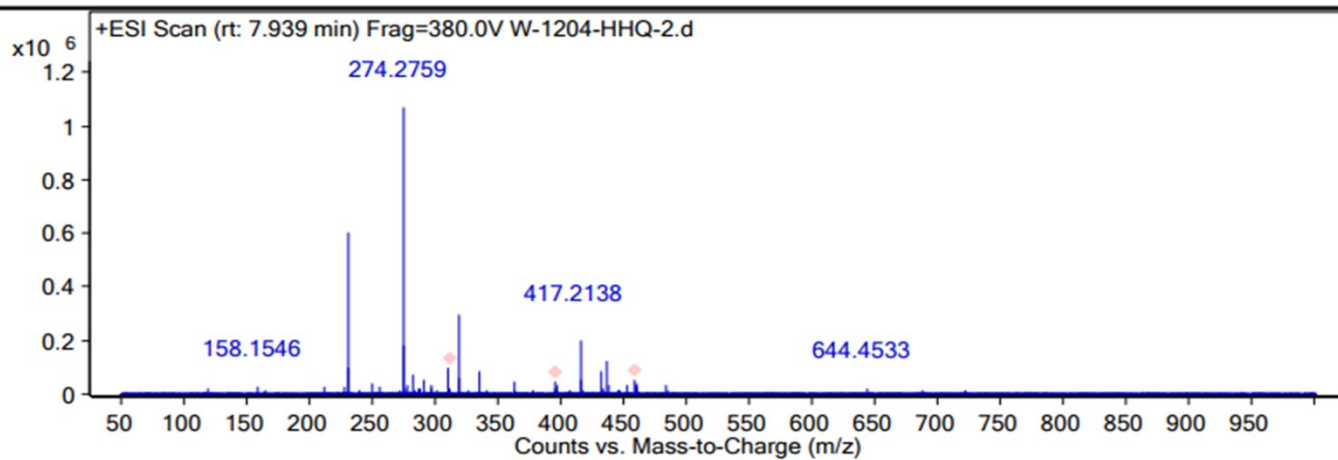
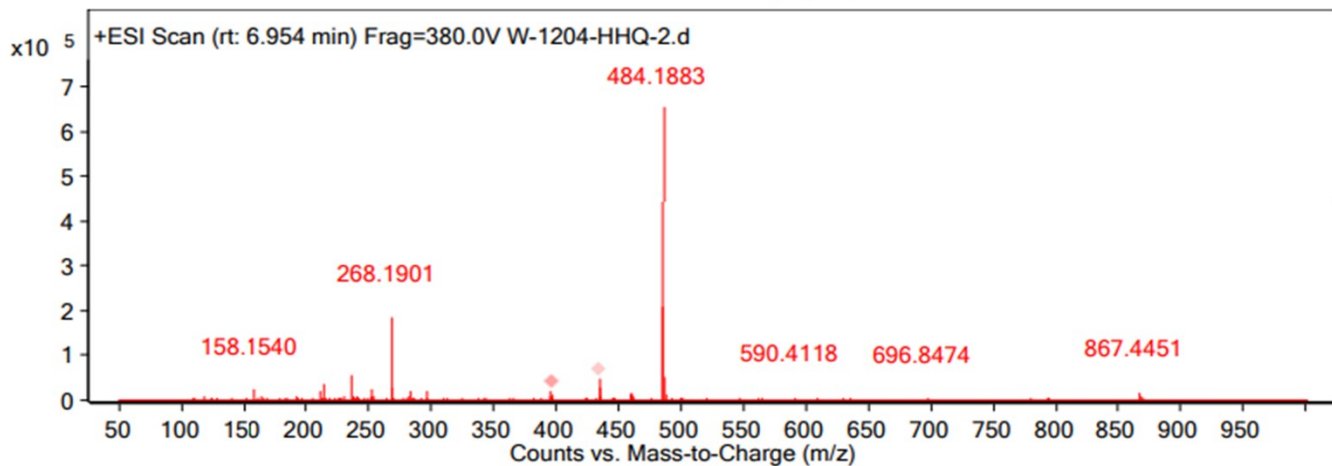
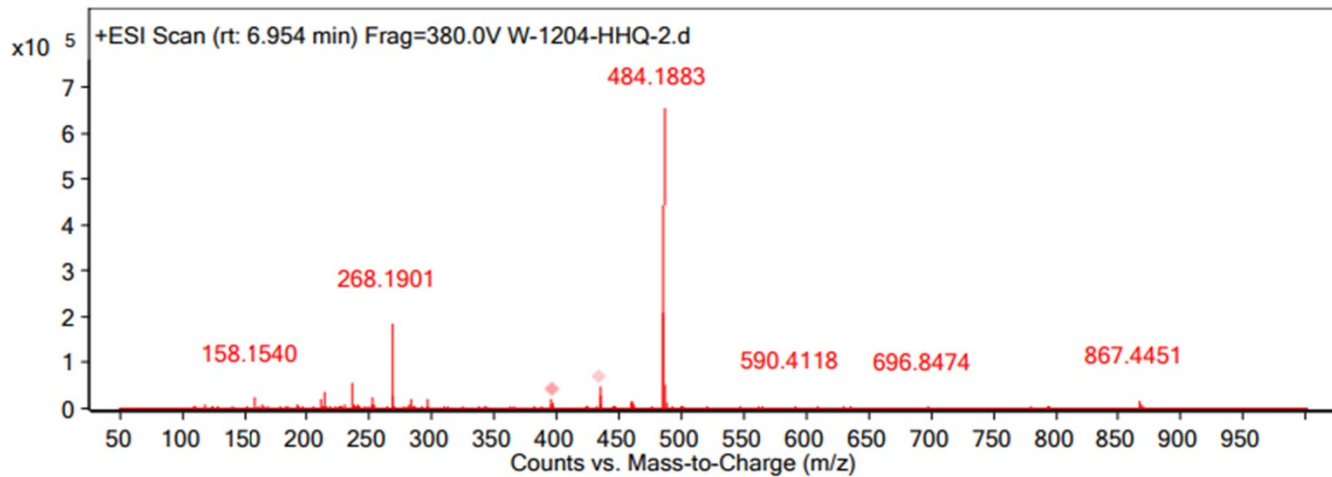
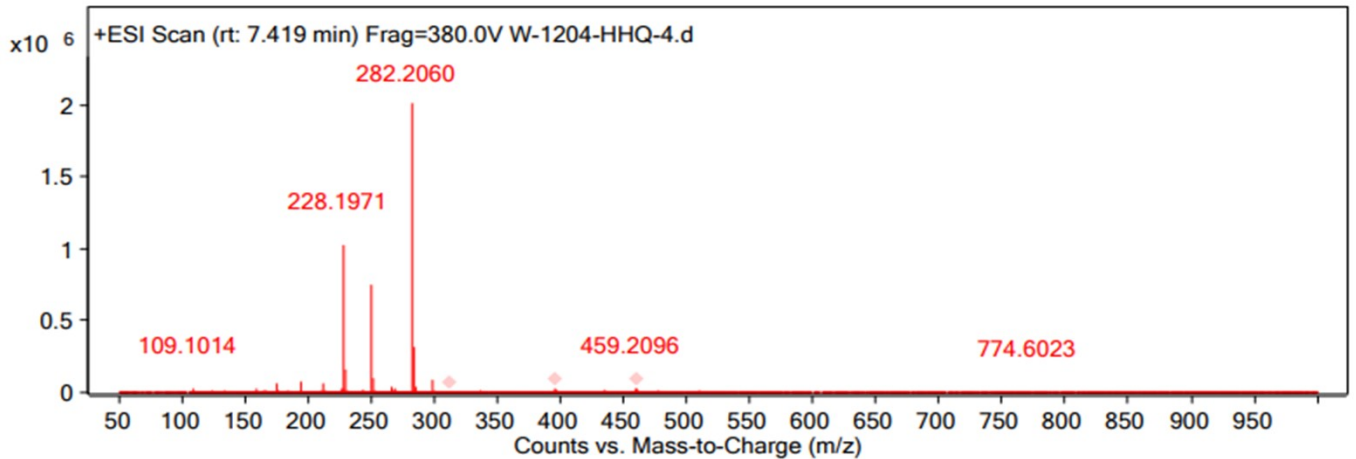
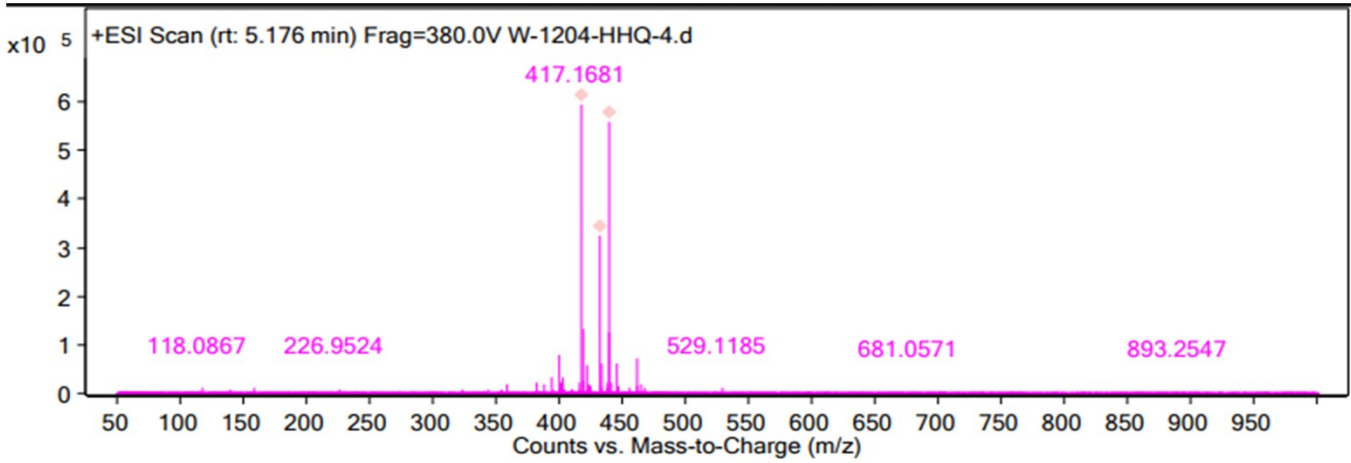
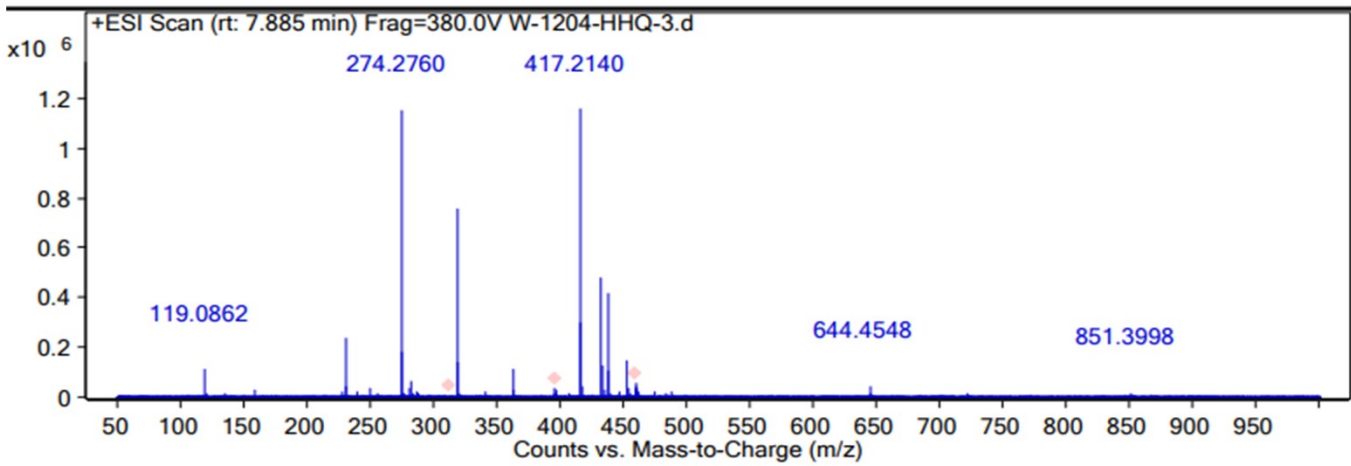
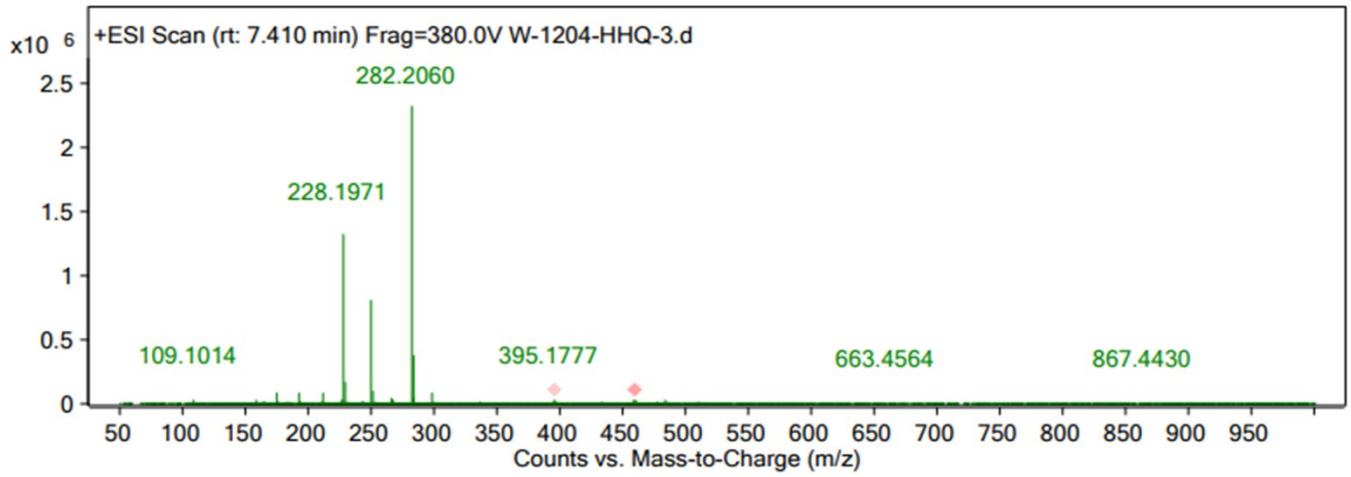


Fig. S6. dark adsorption of TCH on Ti_3C_2 , $ZnFe_2O_4$ and 0.25/1 $Ti_3C_2/ZnFe_2O_4$ photocatalytic materials.







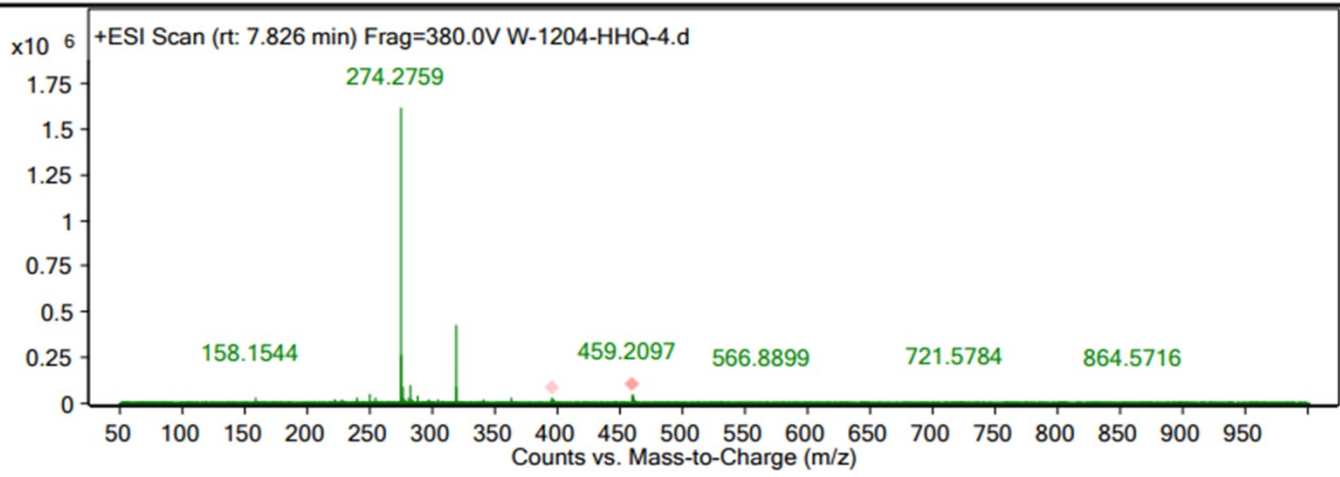


Fig. S7. Mass spectras of degradation intermediates of TCH.

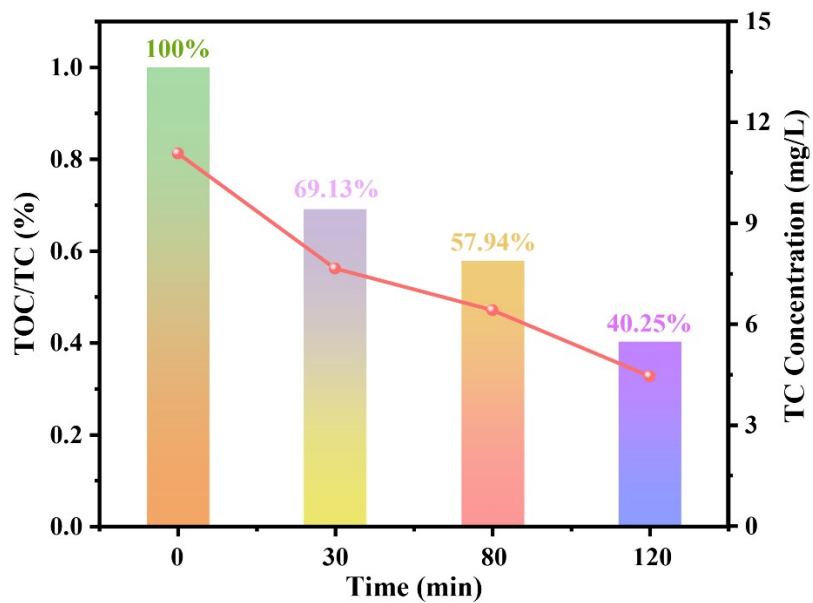


Fig. S8. TOC value of 0.25/1 $\text{Ti}_3\text{C}_2/\text{ZnFe}_2\text{O}_4$ versus TCH at different times.

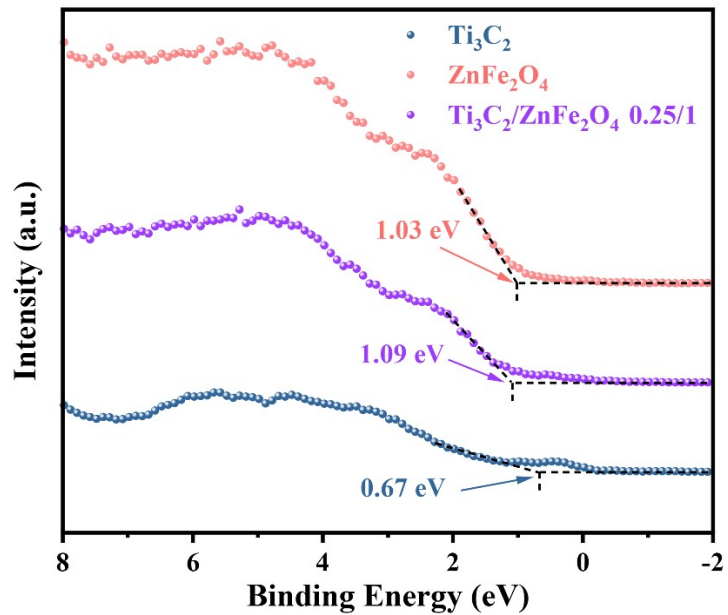


Fig. S9. VB-XPS spectra of Ti_3C_2 , ZnFe_2O_4 and the 0.25/1 $\text{Ti}_3\text{C}_2/\text{ZnFe}_2\text{O}_4$ photocatalyst.

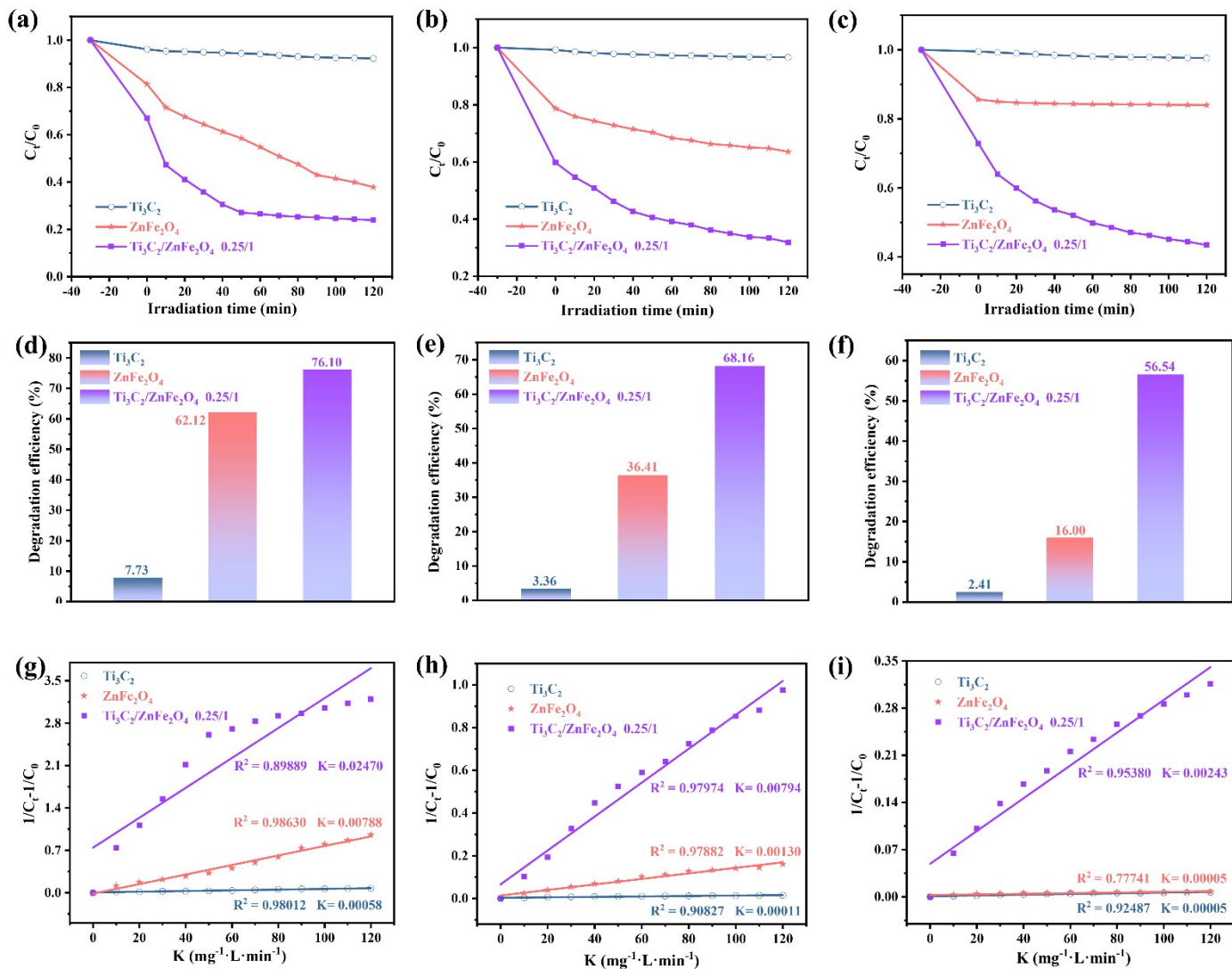


Fig. S10. The degradation curves of water pollutants (a) malachite green, (b) xylene orange and (c) chlortetracycline hydrochloride under visible light and their corresponding degradation efficiency histogram (d-f) and fitting curve of pseudo-second-order kinetics; and (g-i) were studied using 0.25/1 $\text{Ti}_3\text{C}_2/\text{ZnFe}_2\text{O}_4$ as photocatalyst.

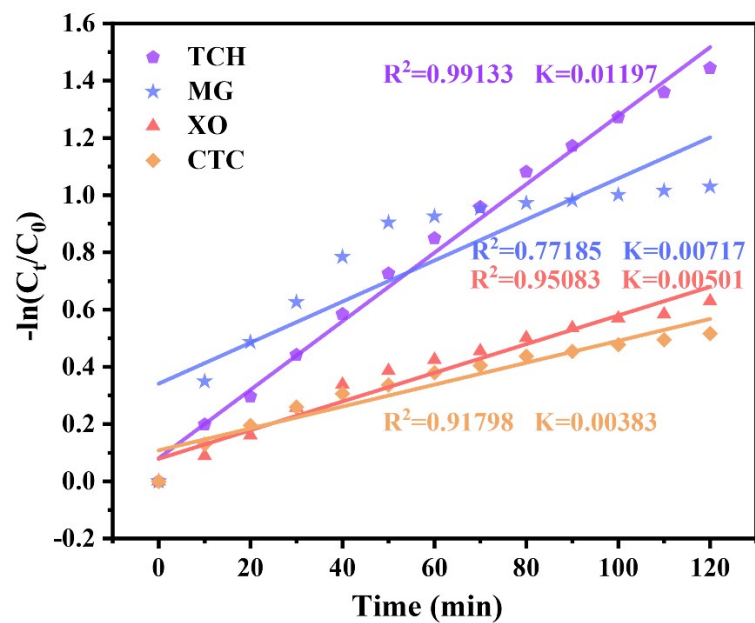


Fig. S11. Fitting curve of pseudo-first-order kinetics.

Table S1: Specific surface area, pore size and pore volume of as-prepared samples.

Samples	BET Surface Area (m ² /g)	Pore Volume (cm ³ /g)	Pore Size (nm)
Ti ₃ C ₂	40.534	0.107	3.704
ZnFe ₂ O ₄	238.159	0.455	7.726
Ti ₃ C ₂ /ZnFe ₂ O ₄	130.858	0.202	5.589

Table S2: The double exponential decay fitting data of the samples and the detailed parameters of the decay life.

Material	$\tau_1 (ns)$	$\tau_2 (ns)$	B_1	B_2	$\tau_{av} (ns)$
Ti ₃ C ₂	15.94386	1.242467	0.4271554	725.6191	1.353
ZnFe ₂ O ₄	15.74716	1.239377	0.9200619	795.202	1.450
0.25/1 Ti ₃ C ₂ /ZnFe ₂ O ₄	16.01142	1.315384	2.05093	873.8648	1.724

$$C(t) = \sum_{i=1,2} B_i \exp(-t / \tau_i)$$

$$\tau_{av} = \frac{\sum_{i=1}^2 B_i \tau_i^2}{\sum_{i=1}^2 B_i \tau_i}$$

Table S3: Different catalysts in visible decline rate of the degradation of TCH, kinetic constants and correlation coefficient.

Catalysts	Degradation efficiency (%)	Kinetic equation	Kinetic constant K (min ⁻¹)	Correlation coefficient
None	0.644	$y = 2.48885 \times 10^{-5}x + 0.00249$	0.000025	0.41844
Ti ₃ C ₂	7.729	$y = 3.40763 \times 10^{-4}x + 0.00258$	0.00034	0.98219
ZnFe ₂ O ₄	62.662	$y = 0.00579x + 0.02533$	0.00579	0.99432
1.5/1 Ti ₃ C ₂ /ZnFe ₂ O ₄	55.501	$y = 0.00414x + 0.04215$	0.00414	0.97003
1/1 Ti ₃ C ₂ /ZnFe ₂ O ₄	64.161	$y = 0.00481x + 0.03567$	0.00481	0.98235
0.5/1 Ti ₃ C ₂ /ZnFe ₂ O ₄	82.248	$y = 0.01028x + 0.09495$	0.01028	0.98693
0.25/1 Ti ₃ C ₂ /ZnFe ₂ O ₄	87.097	$y = 0.01197x + 0.08034$	0.01197	0.99055
0.2/1 Ti ₃ C ₂ /ZnFe ₂ O ₄	70.505	$y = 0.00678x + 0.08696$	0.00678	0.97791

Table S4: Comparison of reports on photocatalytic degradation of pollutants.

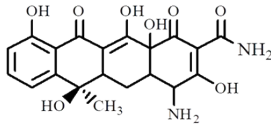
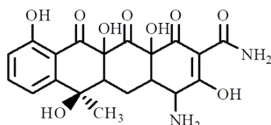
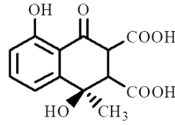
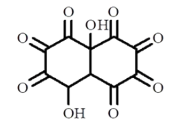
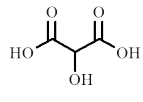
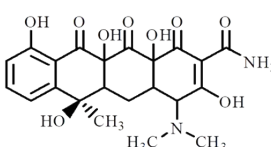
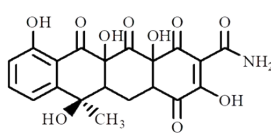
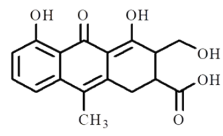
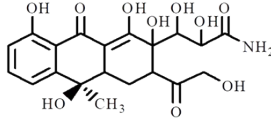
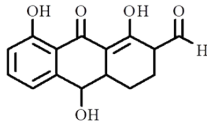
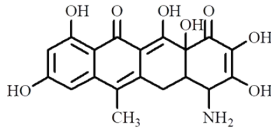
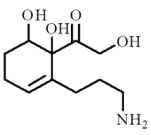
Photocatalyst	Pollutant /Conc. mg·L ⁻¹	V(aq)/ mL	Dose/ mg	Visible light source	Response time/min	Degradation/ %	Ref
ZnFe ₂ O ₄ /CuWO ₄	TC/40	50	40	300 W Xe lamp	150	86	4
CuBi ₂ O ₄ /ZnFe ₂ O ₄	TC/20	100	100	300 W Xe lamp	120	80.16	5
ZnFe ₂ O ₄ /Sepiolite	TC/20	100	100	300 W Xe lamp	180	93.6	6
CdS/ZnFe ₂ O ₄	MB/5; RhB/30; MO/20	20	20	500 W Xe lamp	50	78; 95; 72	7
ZnFe ₂ O ₄ /ZnO	MB/20; MO/20	100	50	500 W halogen lamp	300	91; 99	8
Ag/ZnFe ₂ O ₄ /Ag/ BiTa _{1-x} V _x O ₄	SAM/10	25	25	500 W Xe lamp	360	100	9
ZnFe ₂ O ₄ /C/MnO ₂ / BiOI	MO/10; RhB/10	65	25	300 W Xe lamp	120	90; 94	10
ZnFe ₂ O ₄ /BiVO ₄ / g-C ₃ N ₄	LFX/25	300	150	300 W Xe lamp	105	82	11
ZnIn ₂ S ₄ /ZnFe ₂ O ₄	RhB/20; Cr(VI)/10	50	10; 15	300 W Xe lamp	8; 20	99.6; 96.6	12
ZnFe ₂ O ₄ / Na-bentonite	RhB/10; Cr(VI)/50	100	100	350 W Xe lamp	120	88.6; 94.2	13
Fe-C ₃ N ₄ / Ti ₃ C ₂	TC/20	50	20	280 W Xe lamp	180	86.8	14
BiOBr/Bi ₂ MoO ₆ / Ti ₃ C ₂ /MMTex	LEV/5	50	20	500 W Xe lamp	120	99	15
ZnO/Ti ₃ C ₂	MO/10	300	300	300 W Xe lamp	60	86.8	16
Ti ₃ C ₂ MXene/ CaIn ₂ S ₄	Cr(VI)/40	100	20	300 W Xe lamp	120	98.94	17
Ti ₃ C ₂ MXene/ SnS ₂	Cr(VI)/50	50	25	Xe lamp	60	90.2	18
Bi ₃ O ₄ Br/Ti ₃ C ₂	BPA/10	100	50	300 W Xe lamp	60	91.26	19
Cs ₂ AgBiBr ₆ / Ti ₃ C ₂ Tx	RhB/30	30	20	300 W Xe lamp	70	100	20
Ti ₃ C ₂ /ZnFe ₂ O ₄	TCH/20; MG/20; XO/20; CTC/20	100	20	300 W Xe lamp	120	87.1; 76.1; 68.2; 56.5	This work

TC/TCH: Tetracycline; MB: Methylene blue; RhB: Rhodamine B; MO: Methyl orange; SAM: Sulfonamide;

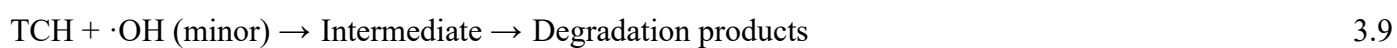
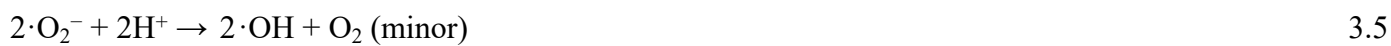
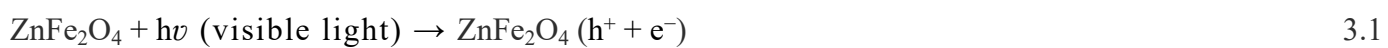
LFX: Lomefloxacin; Cr(VI): Hexavalent Chromium; LEV: Levofloxacin; BPA: Bisphenol A; MG:

Malachite green; XO: Xylenol orange; CTC: Chlortetracycline

Table S5: The possible intermediates products of TCH degradation.

Serial number	Formula	m/z	Potential structure
P1	$C_{20}H_{20}N_2O_{10}$	417.16	
P4	$C_{20}H_{20}N_2O_9$	433.28	
P8	$C_{13}H_{12}O_7$	282.20	
P9	$C_{10}H_4O_9$	268.19	
P10	$C_3H_4O_5$	119.08	
P2	$C_{22}H_{24}N_2O_9$	461.15	
P5	$C_{20}H_{17}NO_{10}$	432.24	
P6	$C_{17}H_{16}O_6$	318.30	
P7	$C_{20}H_{25}NO_{10}$	439.15	
P11	$C_{15}H_{14}O_5$	274.27	
P3	$C_{19}H_{17}NO_8$	388.25	
P12	$C_{11}H_{19}NO_4$	230.25	

Equation S1:



References:

1. B. Tan, Y. Fang, Q. Chen, X. Ao and Y. Cao, *J. Colloid Interface Sci.*, 2021, **601**, 581–593.
2. P. Yuhui, D. Lianwen, Z. Pin, G. Xiaohui, H. Shengxiang, F. Shuguang, Q. Ting and L. Chen, *J. Magn. Magn. Mater.*, 2021, **541**, 168544.
3. J. R. Sandemann, T. B. E. Grønbech, K. A. H. Støckler, F. Ye, B. C. Chakoumakos and B. B. Iversen, *Adv. Mater.*, 2022, **35**, 2207152.
4. J. Luo, Y. Wu, X. Chen, T. He, Y. Zeng, G. Wang, Y. Wang, Y. Zhao and Z. Chen, *J. Alloys Compd.*, 2022, **884**, 161292.
5. K. Song, C. Zhang, Y. Zhang, G. Yu, M. Zhang, Y. Zhang, L. Qiao, M. Liu, N. Yin, Y. Zhao and Y. Tao, *J. Photochem. Photobiol. A Chem.*, 2022, **433**, 114122.
6. C. Zhang, X. Han, F. Wang, L. Wang and J. Liang, *Front. Chem.*, 2021, **9**, 736369.
7. L. Zou, H. Wang, X. Jiang, G. Yuan and X. Wang, *Solar Energy*, 2020, **195**, 271–277.
8. R. Rameshbabu, N. Kumar, A. Karthigeeyan and B. Neppolian, *Materials Chemistry and Physics*, 2016, **181**, 106–115.
9. R. Wang, J. Tang, X. Zhang, D. Wang, X. Wang, S. Xue, Z. Zhang and D. D. Dionysiou, *J. Hazard. Mater.*, 2019, **375**, 161–173.
10. M. Ma, Y. Chen, J. Jiang, Y. Bi, Z. Liao and Y. Ma, *Environ. Sci. Pollut. Res.*, 2022, **29**, 63233–63247.
11. H. B. Truong, B. T. Huy, S. K. Ray, G. Gyawali, Y.-I. Lee, J. Cho and J. Hur, *Chemosphere*, 2022, **299**, 134320.
12. Q. Gao, Z. Wang, J. Li, B. Liu and C. Liu, *Environ. Sci. Pollut. Res.*, 2022, **30**, 16438–16448.
13. Y. Guo, Y. Guo, D. Tang, Y. Liu, X. Wang, P. Li and G. Wang, *J. Alloys Compd.*, 2019, **781**, 1101–1109.
14. Z. Huo, Y. Liao, Y. He, Y. Zhang, X. Liao, Q. Zhang, H. Wu, J. Shi, G. Wen, H. Su and S. Yao, *Front. Chem.*, 2022, **10**, 865847.
15. L. Kun, W. Linxing, F. Tian, Z. Hanbing, L. Caimei, T. Zhangfa, Y. Yang and P. Yuan, *J. Chem. Eng. Data*, 2023, **457**, 141271.
16. Z. Bin, N. Xutao and L. Linfang, *J. Alloys Compd.*, 2023, **963**, 171309.
17. L. Chao, X. Wen, L. Xingyu, W. Qiang, H. Jiawei, Z. Siyuan, X. Jianguang, Z. Qinfang and Z. Zhigang, *Journal of Materials Science & Technology*, 2023, **161**, 123–135.
18. T. Yunmeng, W. Chengquan, Z. Qi, C. Haining, L. Yue, W. Kun, W. Jie, L. Lingliang and Q. Jing, *Sens. Actuators B Chem.*, 2023, **382**, 133496.
19. Z. Huiqi, M. Xiaorong, Y. Yingzi, C. Jin and H. Shanshan, *J. Environ. Chem. Eng.*, 2023, **11**, 110064.

20. C. Shanshan, C. Xu, W. Meng, L. Gaoqiang, Q. Xiaofeng, T. Yongtao, J. Mochen, H. Yanbing, W. Di, L. Xinjian and S. Zhifeng, *Appl. Surf. Sci.*, 2023, **621**, 156877.